Photochemical & Photobiological Sciences

Accepted Manuscript

This article can be cited before page numbers have been issued, to do this please use: L. Han, R. Kang, X. Zu, Y. Cui and J. Gao, *Photochem. Photobiol. Sci.*, 2015, DOI: 10.1039/C5PP00216H.

ROYAL SOCIETY OF CHEMISTRY

www.rsc.org/pps

View Article Online
DOI: 10.1039/C5PP00216H

Journal Name

ARTICLE

Novel coumarin sensitizers based on 2-(thiophen-2-yl)thiazole π-bridge for dye-sensitized solar cell

Received 00th January 20xx,
Accepted 00th January 20xx

DOI: 10.1039/x0xx00000x

www.rsc.org/

Liang Han, Rui Kang, Xiaoyan Zu, Yanhong Cui and Jianrong Gao*

2-(Thiophen-2-yl)thiazole was introduced as a π-bridge into diethylamino coumarin and novel coumarin sensitizers were synthesized with cyanoacrylic acid or rhodanine acetic acid as electron acceptor. Their light-harvesting capabilities and photovoltaic performance were investigated and compared with those of the similar sensitizer bearing phenylthiophene bridge. Replacement of benzene in the π-bridge with thiazole cycle contributes to the improvement of light-harvesting capability and hence superior J_{SC}. 7-Diethylamino coumarin dye with 2-(thiophen-2-yl)thiazole bridge and cyanoacrylic acid acceptor shows the most efficient photoelectricity conversion efficiency which has the maximum value of 4.78% (V_{OC} = 690 mV, J_{SC} = 9.79 mA/cm^2, and ff = 0.71) under simulated AM 1.5 G irradiation (100 mW/cm^2).

1.Introduction

The development and utilization of solar energy have been one of the most important scientific and technological challenges in recent years. The solar cell is a promising approach to convert light into electrical energy through photovoltaic process. [1] The commercially available solar cells are mainly composed of inorganic silicon semiconductors which need silicon with great purity and accordingly high cost. [2] Therefore, hybrid solar cells characteristic of low material cost, easy manufacturing process and flexibility in the scaling processes, appear to be a good alternative to crystalline silicon-based photovoltaics.[3,4] In various hybrid solar cells, dye sensitized solar cells (DSSC) have attracted extensive interests and are on the verge of commercialization.[5]

In DSSC, sensitizing dyes play a critical role in the achievement of high efficiency and long-term durability. A sensitizer is a dye with a broad absorption spectrum and a high molar extinction coefficient, which has strong interaction with semiconductor surface through functionality. [6-8] A few Ru (II) complexes have been reported to be the sensitizers with high photoelectric conversion efficiency. The most famous Ru (II) complexes are bis(tetrabutylammonium)-cis-di(thiocyanato)-bis(4,4'-dicarboxy-2,2'-bipyridine)ruthenium (II) (N719 dye) and trithiocyanato-(4,4',4''-tricarboxy-2,2':6',2''-terpyridine) ruthenium (II) (black dye), achieving a high photoelectric conversion yield (η) of > 11% under AM 1.5 G irradiation.[9,10] However, Ru (II) complexes suffer the disadvantages of the rarity of ruthenium metal in the earth's crust, tricky synthesis, and purification steps. Therefore, metal-free organic sensitizing dyes have called great attention for their large diversity in the molecular structure, simple preparation, and purification process at lower cost.[11] Typical metal-free organic sensitizers are based on a donor-π bridge-acceptor system (D-π-A) to achieve effective charge separation and transfer. Many electron-rich compounds have been found to be the desirable donor for metal-free organic sensitizers, such as triarylamine,[12] coumarin,[13] indoline,[14,15] carbazole,[16] and phenothiazine/ phenoxazine.[17,18]

Coumarin derivatives are characterized with good photoresponse in the visible region, good long-term stability, and appropriate lowest unoccupied molecular orbital (LUMO) levels matching with the conduction band of TiO_2, which brings coumarin compound a good candidate for the donor of the sensitizer. Hara designed a series of coumarin dyes with an optimal power conversion efficiency of 8.2% which ranks the highest among the reported coumarin sensitizers.[19] Since introduction of additional donor or acceptor is a better choice to optimize the absorption spectrum than a flexible extended π-bridge, Kim reported novel D-A-π-A coumarin dye containing benzothiadiazole chromophore[20] and Yu et al. synthesized branched coumarin dyes based on a 2D-π-A system to prevent π-aggregation and improve the photovoltaic performance.[21] However, those coumarin sensitizers feature the coumarin donors substituted by rigid nitrogen-containing cycle which are prepared through redundant synthetic process.

In our previous work, we have reported several coumarin sensitizers characteristic of easily available 7-diethylamine coumarin donor. Compound **ZX-1** bearing the diethylamino coumarin donor, thiophene π-bridge and cyanoacrylic acid acceptor was synthesized and achieved the photoelectric conversion efficiency 3.52%.[22] Based on this, we modified the π-conjugation system and selected benzene, biphenyl and

[a] College of Chemical Engineering, Zhejiang University of Technology, Hangzhou, 310032 Email:gjrarticle@163.com
[b]

† Footnotes relating to the title and/or authors should appear here. Electronic Supplementary Information (ESI) available: [details of any supplementary information available should be included here]. See DOI: 10.1039/x0xx00000x

View Article Online
DOI: 10.1039/C5PP00216H

phenylthiophene as π-bridge to synthesize WHB-series coumarin sensitizers.[23] The photovoltaic test indicates that phenylthiophene bridge favors the photovoltage improvement compared with thiophene bridge. However, introduction of the bulky phenyl group weakens the coplanarity of whole molecule and hence the electron transfer, which is not good for the photocurrent. Therefore, **WHB-5** with the diethylamino coumarin donor, phenylthiophene π-bridge and cyanoacrylic acid acceptor gives a litter better power conversion efficiency 3.62%. To improve the electron transfer and the power conversion efficiency, we further changed the phenyl unit with an electron-withdrawing thiazole. Herein, novel coumarin sensitizers with 2-(thiophen-2-yl)-thiazole π-bridge (**Fig. 1**, **ZXY-a** and **ZXY-b**) were synthesized and better efficiency 4.78% was achieved with this molecular engineering.

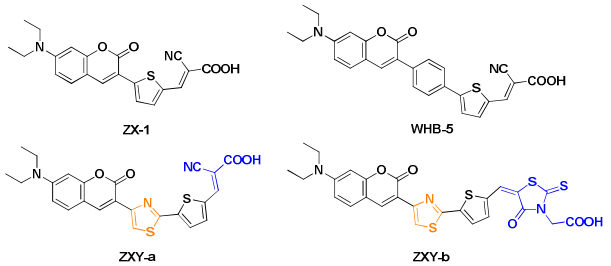

Fig. 1 Structure of the coumain-based dyes

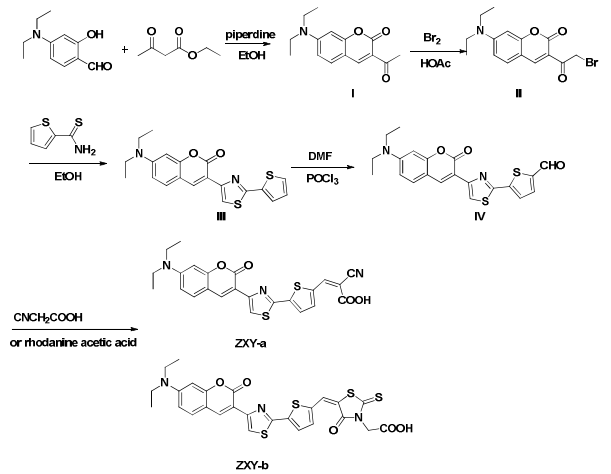

Scheme 1 Syntheses of ZXY-series dyes

2. Experimental sections

2.1 Materials and instruments

Nuclear magnetic resonance spectra were recorded on Bruker Avance III 500 MHz and chemical shifts were expressed in ppm using TMS as an internal standard. Mass spectra were measured using a Waters Xevo Q-Tof Mass Spectrometer. Absorption spectra were measured with SHIMADZU (model UV2550) UV–Vis spectrophotometer. Fluorescence spectra were obtained on a SHIMADZU RF-5301PC spectrofluorometer.

2.2 Fabrication of DSSCs

FTO glass was first cleaned in a detergent solution using an ultrasonic bath for 15 min, and then rinsed with water and ethanol. For the fabrication of photoelectrodes, two different titanium nanoxide pastes were deposited by screen-printing, resulting in the TiO_2 electrodes (0.16 cm^2, with light scattering anatase particles). The total thickness of TiO_2 film was 18 μm. The TiO_2 electrodes were gradually heated under an air flow at 325 °C for 5 min, at 375 °C for 5 min, and at 450 °C for 15 min, and finally, at 500 °C for 15 min. After being cooled to 80 °C, the TiO_2 electrode was immersed into the dye solution in a mixture of MeOH and $CHCl_3$ (V_{MeOH}: V_{CHCl3} = 1:10) and kept at room temperature for 24 h to assure complete dye uptake, which were then rinsed with MeOH to remove excess dye. Meanwhile, the counter electrodes were prepared by screen-printing a 50 nm Pt layers on the cleaned FTO plates. Open cells were fabricated in air by clamping the different photoelectrodes with platinized counter electrodes. The electrolyte used here is composed of the CH_3CN solution of 0.3 M 1-methyl-3-propylimidazolium iodide (MPII), 0.03 M I_2, 0.07 M LiI, 0.1 M guanidinium thiocyanate and 0.4 M 4-tert-butylpyridine (TBP). The active area of DSSCs was 0.16 cm^2.

2.3 Photovoltaic characterization

Photovoltaic performance of the DSSCs was evaluated at AM 1.5 G illumination (100 mW/cm^2; Peccell-L15, Peccell, Japan) using a Keithley digital source meter (Keithley 2601, USA). The incident light intensity was 100 mW/cm^2 calibrated with a standard Si solar cell (BS-520, Japan). The action spectra of monochromatic incident photon-to-current conversion efficiency (IPCE) for solar cell were performed by using a commercial setup (PEC-S20 IPCE Measurement System, Peccell, Japan). Electrochemical impedance spectroscopy (EIS) experiments were conducted using a computer-controlled potentiostat (ZeniumZahner, Germany). The measured frequency ranged from 100 mHz to 1 MHz while the AC amplitude was set to 10 mV. The bias of all EIS measurements was set to the V_{OC} of the corresponding dyes. The cyclic voltammetry were recorded with a computer controlled electrochemical analyzer (IviumStat, Holland) at a constant scan rate of 100 mV/s. Measurement were performed with a three electrode cell in 0.1 M Bu_4NClO_4 N,N-dimethylformamide solution, Pt wire as a counter electrode and an Ag/AgCl reference electrode and calibrated with ferrocene. The HOMO energy versus vacuum (E_{HOMO}) is obtained though the equation: E_{HOMO}= - [E_{OX} + 4.7 eV].[24]

2.4 The detailed experimental procedures and characterization data

*2.4.1 Synthesis of 3-acetyl-7-diethylamino coumarin (**I**)*

Piperidine (1 mL) was added in the solution of 4-diethylamino salicylaldehyde (19.3 g, 100 mmol) and ethyl acetoacetate (18.5 g, 150 mmol) in ethanol (200 mL) and the reactant was refluxed for 5 h. The solvent was removed and the residue was recrystallized with ethanol to give yellow solid (21.3 g, 82.3%). m.p. 150-153 °C [Ref.[23] 150-152 °C]

2.4.2 Synthesis of 3-bromoacetyl-7-diethylamino coumarin (II)

After the addition of hydrobromide (4.5 mL，40.2 mmol) in the solution of compound **I** (5.2 g, 20.1 mmol) in acetic acid (100 mL), liquid bromine (1.1 mL, 20.1 mmol) was slowly

View Article Online
DOI: 10.1039/C5PP00216H

added to the mixture. The reactant was stirred overnight and then filtrated. The filter cake was washed with ethanol and used directly in the next step without further purification.

*2.4.3 Synthesis of 7-diethylamino-3-(2-(thiophen-2-yl)thiazol-4-yl)coumarin (**III**)*

Thiophene-2-carbothioamide (1.5 g, 10.7 mmol) was added in the solution of compound **II** (3.6 g, 10.7 mmol) in ethanol (100 mL) and the reactant was refluxed for 2 h. After being filtrated, the filter cake was recrystallized with ethanol to afford yellow solid (2.5 g, 61.2%). m.p. 169~172 ºC; ^{1}H NMR (500 MHz, $CDCl_3$) δ: 8.74 (s, 1H, thiazole-H), 8.38 (s, 1H, coumarin-H), 7.59 (d, *J* = 2.7 Hz, 1H, thiophene-H), 7.54 (d, *J* = 8.5 Hz, 1H, thiophene-H), 7.46 (d, *J* = 4.1 Hz, 1H, coumarin-H), 7.42-7.39 (m, 1H, thiophene-H), 7.13 (dd, *J* = 5.0, 3.7 Hz, 1H, coumarin-H), 7.05 (d, *J* = 8.4 Hz, 1H, coumarin-8-H), 3.31 (q, *J* = 7.0 Hz, 4H, $C\underline{H}_2CH_3$), 1.14 (t, *J* = 7.1 Hz, 6H, $CH_2C\underline{H}_3$).

*2.4.4 Synthesis of 5-(4-(7-(diethylamino)-2-oxo-2H-chromen-3-yl)thiazol-2-yl)-thiophene-2-carbaldehyde (**IV**)*

After the addition of $POCl_3$ (5 mL), DMF (5 mL) solution was stirred for 0.5 h and then was added into the solution of compound **III** (2.5 g, 6.6 mmol) in DMF (30 mL). After stirred for 8 h at 60 ºC, the mixture was poured into ice water (300 mL) and adjusted to pH = 7 with 10% NaOH solution. After being filtrated, the filter cake was washed with water and ethanol and dried to afford yellow solid (1.22 g, 45.1%). m.p. 215~216 ºC; ^{1}H NMR (500 MHz, $CDCl_3$) δ: 10.19 (s, 1H, CHO), 8.44 (s, 1H, thiazole-H), 7.68 (dd, *J* = 3.8, 1.0 Hz, 1H, coumarin-H), 7.53 (dd, *J* = 5.0, 1.0 Hz, 1H, thiophene-H), 7.42 (d, *J*= 9.0 Hz, 1H, thiophene-H), 7.15 (dd, *J* = 5.0, 3.7 Hz, 1H, coumarin-H), 6.66 (dd, *J* = 8.9, 2.5 Hz, 1H, coumarin-H), 6.55 (d, *J* = 2.4 Hz, 1H, coumarin-H), 3.47 (q, *J* = 7.1 Hz, 4H, $C\underline{H}_2CH_3$), 1.25 (t, *J* = 7.1 Hz, 6H, $CH_2C\underline{H}_3$)

*2.4.5 Synthesis of 2-cyano-3-(5-(4-(7-(diethylamino)-2-oxo-2H-chromen-3-yl)-thiazol-2-yl)thiophen-2-yl)acrylic acid (**ZXY-a**)*

Compound **IV** (0.2 g, 0.5 mmol) and cyanoacetic acid (0.085 g, 1.0 mmol) were dissolved in acetonitrile (5 mL) and then piperidine (0.01 mL, 0.1 mmol) was added. The reactant was refluxed for 6 h and cooled. After the filtration, the filter cake was washed with acetonitrile (20 mL×3) and then recrystallized with $CHCl_3$ to give dark red solid (150 mg, 62.9%). m.p. 241~243 ºC; ^{1}H NMR (500 MHz, DMSO-*d*6) δ: 8.29 (s, 1H, C$\underline{H}$=CCN), 8.27 (s, 1H, thiazole-H), 7.98 (dd, *J* = 3.7, 1.0 Hz, 1H, thiophene-H), 7.96 (dd, *J* = 5.0, 0.9 Hz, 1H, thiophene-H), 7.62 (d, *J* = 9.0 Hz, 1H, coumarin-H), 7.29 (dd, *J* = 5.0, 3.8 Hz, 1H, coumarin-H), 6.81 (dd, *J* = 9.0, 2.4 Hz, 1H, coumarin-H), 6.64 (d, *J* = 2.3 Hz, 1H, coumarin-H), 3.50 (q, *J* = 7.0 Hz, 4H, $C\underline{H}_2CH_3$), 1.17 (t, *J* = 7.0 Hz, 6H, $CH_2C\underline{H}_3$); HR-ESI-MS for $C_{24}H_{19}N_3O_4S_2$: Found: 476.0749 [M-H]$^-$; Calcd. 477.0817.

*2.4.6 Synthesis of 2-(5-((5-(4-(7-(diethylamino)-2-oxo-2H-chromen-3-yl)thiazol-2-yl)thiophen-2-yl)methylene)-4-oxo-2-thioxthiazolidin-3-yl)acetic acid (**ZXY-b**)*

Compound **IV** (0.3 g, 0.73 mmol) and rhodanine acetic acid (0.28 g, 1.46 mmol) were dissolved in acetonitrile (7 mL) and then piperidine (0.01 mL, 0.1 mmol) was added. The reactant was refluxed for 6 h and cooled. After the filtration, the filter cake was washed with acetonitrile (20 mL × 3) and then recrystallized with $CHCl_3$ to give dark red solid (170 mg, 40 %). m.p. 249~250 ºC; ^{1}H NMR (500 MHz, DMSO-*d*6) δ: 13.49 (bs, 1H, COO$\underline{H}$), 8.28 (s, 1H, thiazole-H), 8.01 (dd, *J* = 3.5, 1.0 Hz, 1H, thiophene-H), 7.97 (s, 1H, C$\underline{H}$=C), 7.93 (dd, *J* = 5.0, 1.1 Hz, 1H, thiophene-H), 7.63 (d, *J* = 9.0 Hz, 1H, coumarin-H), 7.29 (dd, *J* = 5.0, 3.8 Hz, 1H, coumarin-H), 6.80 (dd, *J* = 9.0, 2.4 Hz, 1H, coumarin-H), 6.65 (d, *J* = 2.3 Hz, 1H, coumarin-H), 4.73 (s, 2H, $C\underline{H}_2COOH$), 3.50 (q, *J* = 7.0 Hz, 4H, $C\underline{H}_2CH_3$), 1.17 (t, *J* = 7.0 Hz, 6H, $CH_2C\underline{H}_3$); HR-ESI-MS for $C_{26}H_{21}N_3O_5S_4$: Found: 582.0294 [M-H]$^-$; Calcd. 583.0364

3. Results and Discussion

3.1 Synthesis

Diethylaminosalicylaldehyde reacted with ethyl acetoacetate to afford 3-acetyl-7-diethylaminocoumarin **I** which was brominated at the acetyl group to produce the bromide **II**. The thiazole ring was formed through Hantzsch synthesis between the bromide **II** and thiophene-2-carbothioamide to give 7-diethylamino-3-(2-(thiophen-2-yl)thiazol-4-yl)coumarin **III**. The aldehyde group was introduced into the thiophene of compound **III** through Vilsmeier reaction and then condensed with cyanoacetic acid or rhodanine acetic acid to yield the target compounds **ZXY-a** and **ZXY-b**.

3.2 Optical properties

The UV absorption of **ZXY-a** and **ZXY-b** in CH_3OH-$CHCl_3$ cosolvent were shown in **Fig. 2**(a) and the corresponding data were listed in **Table 1** with those of **WHB-5** for comparison. **ZXY-a** and **ZXY-b** display two distinct maximum absorption peaks: one occurs at about 400 nm and is caused by π-π* transition; another peak locates at 460-490 nm and may be attributed to intramolecular charge transfer (ICT) from the diethylamino coumarin donor to the acceptor bearing carboxyl group through 2-(thiophen-2-yl)thiazole π-bridge. Due to the expansion of π-conjugation system, **ZXY-b** with rhodanine acetic acid acceptor exhibits longer maximum absorption wavelength and larger molar extinction coefficient than **ZXY-a** with cyanoacrylic acid acceptor. The ICT absorption peak of **ZXY-a** shifts bathochormically when compared to that of **WHB-5**, which indicates the replacement of the phenyl ring with the electron-withdrawing thiazole ring, favors the intramolecular charge transfer.

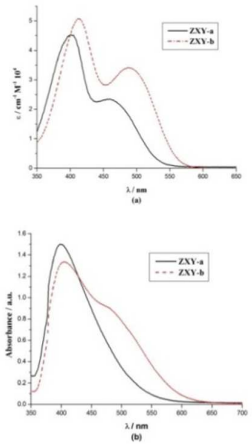

Fig.2 UV spectra of coumarin sensitizing dyes
(a) in CH_3OH-$CHCl_3$ cosolvent(VCH_3OH:$VCHCl_3$=1:10);
(b) on sensitized TiO_2 electrode (1.0 μm in thickness)

View Article Online
DOI: 10.1039/C5PP00216H

Table 1 Optical properties of coumarin sensitizing dyes

Compd	λ_{max} [a] / (nm)	ε [a] / ($M^{-1}\cdot cm^{-1}$)	λ_{max} [b] / (nm)	λ_{max} [c] / (nm)
ZXY-a	401, 460	45333, 23433	400	581
ZXY-b	413, 489	50800, 34167	405	607
WHB-5	438	37300	432	500

[a] maximum absorption wavelength λ_{max} and molar extinction coefficient at λ_{max} of dyes measured in CH_3OH-$CHCl_3$ cosolvent (V_{CH3OH}: V_{CHCl3}=1:10); [b] maximum absorption wavelength λ_{max} of dyes on sensitized TiO_2 electrodes; [c] maximum emission wavelength measured in CH_3OH-$CHCl_3$ cosolvent (V_{CH3OH}: V_{CHCl3}=1:10)

Generally, dye molecules are deprotonated on TiO_2 film to form a carboxylate-TiO_2 unit which may facilitate the charge injection and at the same time lead to the blue shift of the absorption peak. Moreover, an occurrence of dye aggregation on TiO_2 film induces the broadening of the absorption spectrum and the blue shift (H-aggregate) or red shift (J-aggregate) of the absorption peak. **Fig. 2**(b) listed the absorption spectra of **ZXY-a** and **ZXY-b** on TiO_2 film and the hypsochromical shift of the maximum absorption peak was observed. On the other hand, the onset of the absorption spectra has been pushed only about 50 nm further while the whole spectra region appears not be broadened on TiO_2 film when compared with that in solution. Therefore, we speculate the hypsochromical shift of the absorption peak may be mainly ascribed to the deprotonation of the carboxylic acid which lowers the electron-withdrawing ability of the carboxylic acid and accordingly weakens the ICT.

3.3 Computational studies

To gain an insight into the relationship between the structure and the photophysical properties, the ground-state geometries of coumarin dyes have been optimized by DFT with the Gaussian package, using the hybrid B3LYP functional and the standard 6-31G(d) basis set.

The fully optimized geometrical structure of **ZXY-a** is shown in **Fig. 3** and also listed that of **WHB-5** for comparison. In **WHB-5** molecule, large deviation from coplanarity between the coumarin and benzene is observed. The presence of the benzene ring induces large distortion and weakens the conjugation of the whole molecule. With the replacement of benzene by thiazole of small size, **ZXY-a** molecule exhibits improved planarity configuration, which favors the intramolecular charge transfer and accordingly the light absorptivity. On the other hand, the introduction of the electron-withdrawing thiazole may contribute to the adjustment of energy level. As shown in **Table 2**, when thiazole ring was introduced to replace the benzene ring, the HOMO-1 and LUMO energy level were lowered down while the LUMO energy level was reduced more than the HOMO-1 energy level. Since the transition from the HOMO-1 to LUMO plays the leading role after the photoexcitation in these coumarin sensitizers (*vide infra*), the E_{gap} between the HOMO-1 and LUMO is actually reduced by the introduction of the thiazole ring. Therefore, the replacement of benzene by thiazole benefits the molecular coplanarity and small energy gap, which leads to longer maximum absorption wavelength of **ZXY-a** than that of **WHB-5**.

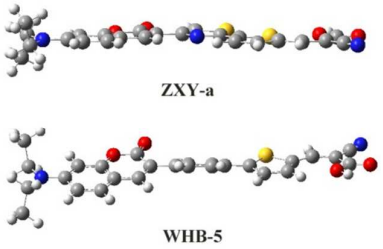

Fig.3 Optimized geometries (side view) of **ZXY-a** and **WHB-5** at the B3LYP/6-31G(d) level

Table 2 Energy level data of **ZXY-a** and **WHB-5** at the B3LYP/6-31G(d) level

Molecule	E_{HOMO-1} / eV	E_{HOMO} / eV	E_{LUMO} / eV	Egap* / eV
ZXY-a	-6.17	-5.40	-2.93	3.24
WHB-5	-6.09	-5.42	-2.70	3.39

*Egap= E_{LUMO} - E_{HOMO-1}

Fig. 4 listed frontier molecular orbitals of coumarin dyes. As can be seen, the HOMOs of ZXY-sensitizers are mostly delocalized at the coumarin donor and the LUMOs are mainly composed of the electron-withdrawing acceptor, while the HOMO-1 of ZXY-sensitizers are delocalized over the whole molecules. Since the overlap of the HOMO-1 with LUMO is better than that of the HOMO, the electron transition after photoexcitation from the HOMO-1 to LUMO in ZXY-sensitizers may be easier than that from the HOMO to LUMO.

Moreover, the energy gap of **ZXY-a** and **ZXY-b** between the HOMO and LUMO shown in **Fig. 5** are 2.47 eV and 2.41 eV, respectively, and the difference 0.06 eV is too small to meet the difference 29 nm of the experimental absorption data. On the other hand, the energy gap of **ZXY-b** between the HOMO-1 and LUMO is 2.95 eV and smaller than that of **ZXY-a** 3.24 eV, which agrees with the red-shifted maximum absorption of the former in **Fig. 2**. Therefore, it also indicates that the electronic transition of ZXY-sensitizers after the photoexcitation is mainly caused by the transition from the HOMO-1 to LUMO.

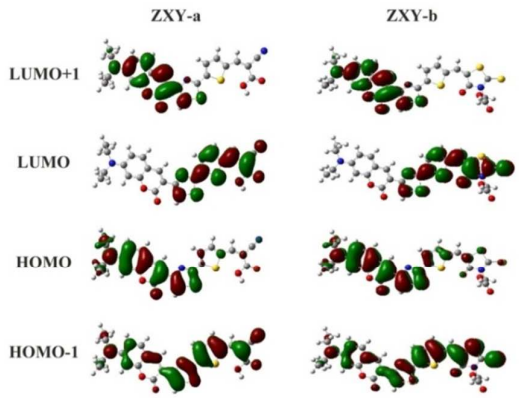

Fig. 4 Frontier molecular orbitals (HOMO-1, HOMO, LUMO, and LUMO+1) of coumarin dyes

View Article Online
DOI: 10.1039/C5PP00216H

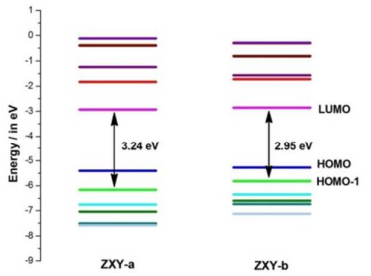

Fig. 5 The energy level of the frontier molecular orbitals of coumarin dyes at B3LYP/6-31G(d)

To further explain the electronic transition after the photoexcitation, the TDDFT calculation is performed at the B3LYP/6-31G(d) level based on the above optimized ground-state geometries of coumarin dyes and the related data are listed in **Table 3**. Two most important electronic transitions are described for each compound: one is the electronic transition with longest absorption wavelength and the other electronic transition has the largest oscillator strength. The absorption peak (408.91 nm) of **ZXY-a** with the maximum oscillator strength corresponds to $S_0 \rightarrow S_2$ transition, and the electrons mainly transfer from the HOMO-1 to LUMO. The calculated UV absorption of **ZXY-b** with the maximum oscillator strength centers at 447.73 nm corresponding to $S_0 \rightarrow S_3$ transition, which is also composed of the electron transfer from the HOMO-1 to LUMO. The results of TDDFT calculation accord with both the suggestion of the frontier molecular orbitals and the experimental absorption data.

3.4 Photovoltaic performance

The IPCE action spectra of DSSCs based on coumarin dyes have been measured under AM 1.5 G irradiation (100 mW/cm^2) and are shown in **Fig. 6**. **ZXY-a** shows a broad IPCE response from 350 to 550 nm with a maximum value of 73% in the plateau region. IPCE is mainly influenced by the light harvesting ability and the overall electron injection efficiency. As can be seen, when compared with **ZXY-a**, **ZXY-b** displays a little broader absorption spectra on TiO_2 film, which indicates **ZXY-b** has similar or even better light harvesting ability than **ZXY-a**. However, **Fig. 6** shows that **ZXY-b** exhibits distinctly inferior IPCE action spectra to **ZXY-a**, which indicates the weak electron injection efficiency of the former. In fact, the presence of methylene group between the carboxylic acid and rhodanine cycle of **ZXY-b** breaks the conjugation system of the whole molecule, which weakens the overlap of the electron density of the dyes with the semiconductor and deteriorates the electron injection into the conduction band of TiO_2.[25, 26] When compared with **WHB-5**, **ZXY-a** also displays superior IPCE spectrum, which demonstrates again the replacement of benzene with thiazole favors charge separation and collection.

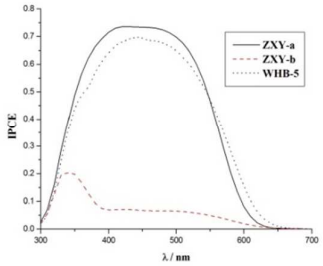

Fig. 6 IPCE curve for DSSCs based on coumarin dyes with 18.0 μm nanocrystalline TiO_2 electrodes

The *J-V* curves of DSSC based on coumarin sensitizing dyes are shown in **Fig. 7** and the corresponding parameters J_{SC}, V_{OC}, *ff* and η are listed in **Table 4**. With a better IPCE spectrum, **ZXY-a** has a short-circuit photocurrent density of 9.79 mA·cm^{-2}, well above of 0.97 mA·cm^{-2} of **ZXY-b** and 7.72 mA·cm^{-2} of **WHB-5**. In addition, the open-circuit photovoltage of **ZXY-a** is higher than that of **ZXY-b** due to the effective electron injection efficiency of the former. Therefore, the optimal photovoltaic performance of 4.78% came from DSSC based on **ZXY-a**, which exhibited a J_{SC} value of 9.79 mA/cm^2, V_{OC} value of 0.69 V, and *ff* value of 0.71.

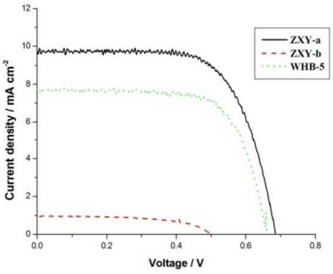

Fig. 7 Current-potential curve (*J-V*) for DSSCs based on coumarin dyes

Table 3 Electronic transition data of coumarin dyes obtained at the TDDFT//B3LYP/6-31G(d) level

Molecule	Electronic transitions	λ_{abs} (nm)	f	Main conf. coefficient*	
ZXY-a	$S_0 \rightarrow S_1$	571.79	0.1415	HOMO→LUMO	0.70386
	$S_0 \rightarrow S_2$	408.91	1.2492	HOMO-1→LUMO	0.63367
ZXY-b	$S_0 \rightarrow S_1$	580.60	0.2390	HOMO→LUMO	0.70259
	$S_0 \rightarrow S_3$	447.73	1.2192	HOMO-1→LUMO	0.68545

*Main conf. coefficient stands for the main composition and the corresponding coefficient of the electron transition after the molecule absorbs the ultraviolet-visible light.

View Article Online
DOI: 10.1039/C5PP00216H

Journal Name

ARTICLE

Table 4 Parameters for DSSCs based on coumarin sensitizing dyes: open-circuit photovoltage V_{OC}, shortcircuit photocurrent density J_{SC}, fill factor *ff*, solar energy-to-electricity conversion efficiency η.

Compd	V_{OC} (V)	J_{SC} (mA·cm^{-2})	*ff*	η%
ZXY-a	0.69	9.79	0.71	4.78
ZXY-b	0.50	0.96	0.69	0.33
WHB-5	0.66	7.72	0.71	3.62

Electrochemical impedance spectroscopy (EIS) measurement provides the charge transfer resistance information of the TiO_2-dye-electrolyte interface. The EIS measurement of ZXY-sensitizers is evaluated in dark and the Nyquist and Bode spectra are shown in **Fig. 8**. In the dark under forward bias, electrons are transported through the mesoscopic TiO_2 network and react with I_3^- and simultaneously I^- is oxidized to I_3^- at the counter electrode (CE).[27] The reaction resistance of DSSCs with a constant phase element (CPE) and resistance (R) is obtained through an equivalent circuit shown in **Fig. 8(c)** using the software (ZSimpWin). In the equivalent circuit, the charge-transfer resistances at the photoanode/electrolyte interface and CE are denoted by R_{ct} and R_{ce} respectively, while R_s represents the overall series resistance. The corresponding parameters R_s and R_{ct} are listed in **Table 5**. Due to the same electrolyte and electrode in the materials and surface area, similar series resistance are observed in these DSSCs. Generally, the semicircle in the frequency 1-1k Hz in the Nyquist diagram corresponds to the electron transfer at the TiO_2/electrolyte interface.[28] The larger the radius of the semicircle, the higher the charge transfer resistance. Larger radius in the Nyquist diagram relates to smaller frequency in the Bode diagram, which means charge recombination is difficult to happen. Compared with **ZXY-a** sensitized DSSC, **ZXY-b** sensitized DSSC displays bigger semicircle in the Nyquist diagram and smaller frequency in the Bode diagram, which means it has larger R_{ct} than **ZXY-a** as shown in **Table 5**. This result was similar to our previous work[22] and the resistance of the DSSC based on **ZXY-b** bearing rhodanine acetic acid acceptor is larger than that of **ZXY-a** bearing

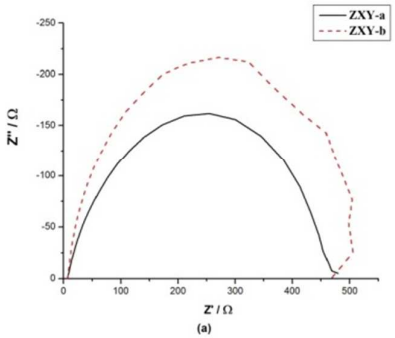

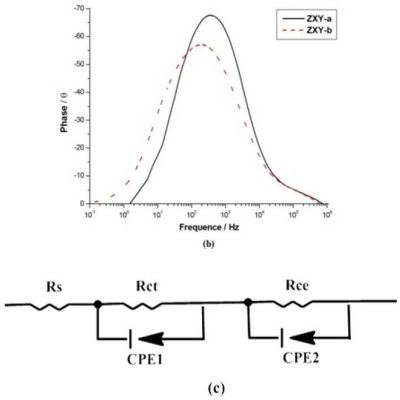

Fig. 8 Electrochemical impedance spectra for DSSCs based on coumarin sensitizing dyes (a) Nyquist plot; (b) Bode plot; (c) equivalent circuits

cyanoacrylic acid acceptor. Large resistance leads to hard charge recombination, which should contribute to the improvement of V_{OC}. In fact, **ZXY-b** sensitized DSSC shows lower V_{OC} than **ZXY-a** sensitized DSSC, which was caused by the inferior charge injection efficiency of the former as suggested by its low J_{SC}, since V_{OC} is mainly determined by both the electron injection efficiency and charge recombination degree.

Table 5 Parameters obtained by fitting the impedance spectra of DSSCs based on coumarin sensitizers using the equivalent circuit

Compd	R_s (Ω)	R_{ct} (Ω)
ZXY-a	6.929	467.3
ZXY-b	6.337	509.1

Conclusions

Two novel coumarin sensitizers were synthesized with diethylamino coumarin as the electron donor, 2-(thiophen-2-yl)thiazole as the π-bridge and cyanoacrylic acid or rhodanine acetic acid as the electron acceptor. Compared with the similar compound with phenylthiophene π-bridge, the replacement of benzene by thiazole cycle favors intramolecular charge transfer and helps the red shift of the maximum absorption. The J_{SC} of **ZXY-a** was improved to 9.79 mA/cm^2 from 7.72 mA/cm^2 of **WHB-5** when shared with the same electron donor and acceptor while just different in π-bridge. In these coumarin

View Article Online
DOI: 10.1039/C5PP00216H

sensitizers, the photovoltaic performance was mainly influenced by the electron injection and **ZXY-b** with rhodanine acetic acid acceptor displayed poor J_{SC} and V_{OC} though with better absorption spectrum and less charge recombination. Therefore, with the replacement of benzene by thiazole, the photoelectricity conversion efficiency was increased to 4.78%.

Acknowledgements

The authors gratefully acknowledge for funding: National Natural Science Foundation of China (21406202); National Natural Science Foundation of China (21176223); and Natural Science Foundation of Zhejiang province (LY13B020012).

Notes and references

1. R. W. Miles, K. M. Hynes and I. Forbes, Photovoltaic solar cells: An overview of state-of-the-art cell development and environmental issues, *Prog. Cryst. Growth Ch.*, 2005, **51**, 1-42.
2. C. Strümpel, M. McCann, G, Beaucarne, V. Arkhipoc, A. Slaoui, V. Švrček, C. del Canizo and I. Tobias, Modifying the solar spectrum to enhance silicon solar cell efficiency-An overview of available materials, *Sol. Energy Mat. Sol. C.*, 2007, **91**, 238-249.
3. M. Grätzel, Recent advances in sensitized mesoscopic solar cells, Accounts Chem. Res., 2009, **42**, 1788-1798.
4. Y. Wang, K. Liu, P. Mukherjee, D. A. Hines, P. Santra, H. Y. Shen, P. Kamat and D. H. Waldeck, Driving charge separation for hybrid solar cells: photo-induced hole transfer in conjugated copolymer and semiconductor nanoparticle assemblies, *Phys. Chem. Chem. Phys.*, 2014, **16**, 5066-5070.
5. A. Hafeldt, G. Boschloo, L. C. Sun, L. Kloo and H. Pettersson, Dye-sensitized solar cells, *Chem. Rev.*, 2010, **110**, 6595-6663.
6. B-G. Kim, K. Chung and J. Kim, Molecular design principle of all-organic dyes for dye-sensitized solar cells, *Chem. Eur. J.*, 2013, **19**, 5220-5230.
7. Y. Z. Wu, W. H. Zhu, Organic sensitizers from D-π-A to D-A-π-A: effect of the internal electron-withdrawing units on molecular absorption, energy levels and photovoltaic performances, *Chem. Soc. Rev.*, 2013, **42**, 2039-2058.
8. J. N. Clifford, E. Nartinez-Ferrero, A. Viterisi and E. Palomares, Sensitizer molecular structure-device efficiency relationship in dye sensitized solar cells, *Chem. Soc. Rev.*, 2011, **40**, 1635-1646.
9. H. Ozawa, Y. Okuyama, H. Arakawa, Dependence of the efficiency improvement of black-dye-based dye-sensitized solar cells on alkyl chain length of quaternary ammonium cations in electrolyte solutions, *Chemphyschem*, 2014, **15**, 1201-1206.
10. C. F. Chi, S. C. Su, I. P. Liu, C. W. Lai and Y. L. Lee. Charge transfer and performance enhancement of dye-sensitized solar cells by utilization of a tandem structure, *J. Phys. Chem. C*, 2014, **118**, 17446-17451
11. A. Mishra, M. K. R. Fischer and P. Bäuerle, Metal-free organic dyes for dye-sensitized solar cells: from structure: property relationships to design rules, *Angew. Chem. Int. Ed.*, 2009, **48**, 2474-2499.
12. A. Baheti, K. R. J. Thomas, C. P. Lee, C. T. Li and K. C. Ho. Organic dyes containing fluoren-9-ylidene chromophores for efficient dye-sensitized solar cells, *J. Mater. Chem. A*, 2014**, 2**, 5766-5779
13. X. G. Liu, J. M. Cole, P. G. Waddel, T. C. Lin, J. Radia and Z. Zeidler, Molecular origins of optoelectronic properties in coumarin dyes: toward designer solar cell and laser applications, *J. Phys. Chem. A*, 2012, **116**, 727-737
14. B. Liu, B. Wang, R. Wang, L. Gao, S. H. Huo, Q. B. Liu, X. Y. Li and W. H. Zhu, Influence of conjugated π-linker in D-D-π-A indoline dyes: towards long-term stable and efficient dye-sensitized solar cells with high photovoltage, *J. Mater. Chem. A*, 2014, **2**, 804-812
15. W. H. Zhu, Y. Z. Wu, S. T. Wang, W. Q. Li, X. Li, J. Chen, Z. S. Wang and H. Tian, Organic D-A- π -A solar cell sensitizers with improved stability and spectral response, *Adv. Funct. Mater.* 2011, **21**, 756-763
16. L. Han, X. Y. Zu, Y. H. Cui, H. B. Wu, Q. Ye and J. R. Gao, Novel D-A-π-A carbazole dyes containing benzothiadiazole chromophores for dye-sensitized solar cells, *Org. Electron.*, 2014, **15**, 1536-1544.
17. Y. Hua, S. Chang, J. He, C. S. Zhang, J. Z. Zhao, T. Chen, W. Y. Wong, W. K. Wong and X. J. Zhu, Molecular engineering of simple phenothiazine-based dyes to modulate dye aggregation, charge recombination, and dye regeneration in highly efficient dye-sensitized solar cells, *Chem. Eur. J.*, 2014, **20**, 6300-6308.
18. H. J. Tan, C. Y. Pan, G, Wang, Y. Y. Wu, Y. P. Zhang, Y. P. Zou, G. P. Yu and M. Zhang, Phenoxazine-based organic dyes with different chromophores for dye-sensitized solar cells, *Org. Electron.*, 2013, **14**, 2795-2801.
19. Z. S. Wang, Y. Cui, Y. Dan-oh, C. Kasada, A. Shinpo and K. Hara, Thiophene-functionalized coumarin dye for efficient dye-sensitized solar cells: electron lifetime improved by coadsorption of deoxycholic acid, *J. Phys. Chem. C*, 2007, **111**, 7224-7230.
20. K. D. Seo, I. T. Choi, Y. G. Park, S. Kang, J. Y. Lee, H. K. Kim, Novel D-A-π-A coumarin dyes containing low band-gap chromophores for dye-sensitised solar cells, *Dyes Pigm.*, 2012, **94**, 469-474.
21. B. Liu, R. Wang, W. Mi, X. Li and H. Yu, Novel branched coumarin dyes for dye-sensitized solar cells: significant improvement in photovoltaic performance by simple structure modification, *J. Mater. Chem.*, 2012, **22**, 15379-15387.
22. L. Han, X. Zhou, Q. Ye, Y. J. Li and J. R. Gao. Synthesis and photoelectric properties of coumarin type sensitizing dyes, *Chin. J. Org. Chem.*, 2013, **33**, 1000-1004.
23. L. Han, H. B. Wu, Y. H. Cui, X. Y. Zu, Q. Ye and J. R. Gao, Synthesis and density functional theory study of novel coumarin-typedyes for dye sensitized solar cells, *J. Photochem. Photobio. A*, 2014, **290**, 54-62.
24. Y. Wang, Z. Xie, G. Gotesman, L. Wang, B. P. Bloom, T. Z. Markus, D. Oron, R. Naaman and D. H. Waldeck. Determination of the electronic energetics of CdTe nanoparticle assemblies on Au electrodes by photoemission, electrochemical, and photocurrent studies, *J. Phys. Chem. C*, 2012, **116**, 17464-17472.
25. B. Liu, W. Q. Li, B. Wang, X. Y. Li, Q. B. Liu, Y. Naruta and W. H. Zhu, Influence of different anchoring groups in indoline dyes for dye-sensitized solar cells: Electron injection, impedance and charge recombination, *J. Power Sources*, 2013, **234**, 139-146.
26. J. Wiberg, T. Marinado, D. P. Hagberg, L. C. Sun, A. Hagfeldt and B. Albinsson, *J. Phys. Chem. C*, 2009, **113**, 3881-3886.
27. Q. Wang, J. E. Moser and M. Grätzel, Electrochemical impedance spectroscopic analysis of dye-sensitized solar cells, *J. Phys. Chem. B*, 2005, **109**, 14945-14953.
28. K. Pan, Y. Z. Dong, C. G. Tian, W. Zhou, G. H. Tian, B. F. Zhao and H. G. Fu, TiO_2-B narrow nanobelt/TiO2 nanoparticle composite photoelectrode for dye-sensitized solar cells, *Eletrochimica Acta*, 2009, **54**, 7350-7356.

View Article Online
DOI: 10.1039/C5PP00216H

Novel coumarin sensitizers based on 2-(thiophen-2-yl)thiazole π-bridge for dye-sensitized solar cell

Liang Han, Rui Kang, Xiaoyan Zu, Yanhong Cui, Jianrong Gao *
(College of Chemical Engineering, Zhejiang University of Technology, Hangzhou, 310032)

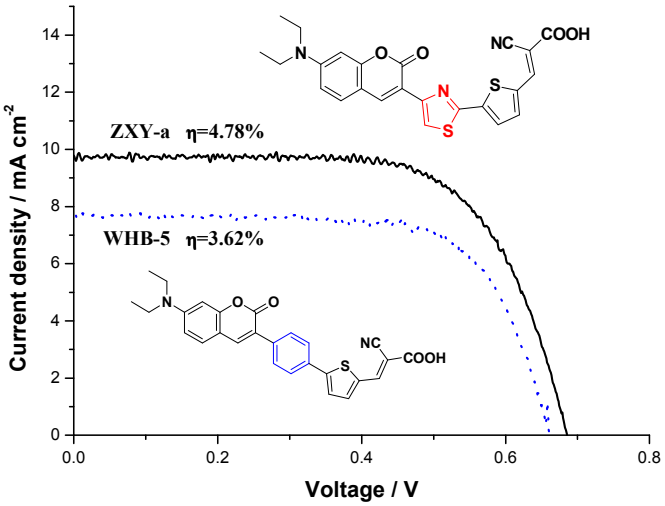

Diethylaminocoumarin dye with 2-(thiophen-2-yl)thiazole bridge and cyanoacrylic acid acceptor was synthesized and showed the photoelectricity conversion efficiency of 4.78% (V_{OC} = 690 mV, J_{SC} = 9.79 mA/cm^2, and *ff* = 0.71) under simulated AM 1.5 irradiation (100 mW/cm^2).

* Corresponding author. Phone: +86 0571 88320891; Email: gjrarticle@163.com